



## Synthesis and Characterization of FLG/Fe<sub>3</sub>O<sub>4</sub> Nanohybrid Supercapacitor

Maria Sarno, Claudia Cirillo, Eleonora Ponticorvo\*, Paolo Ciambelli

Department of Industrial Engineering and Centre NANO\_MATES, University of Salerno  
Via Giovanni Paolo II, 132 - 84084 Fisciano (SA), Italy  
[eponticorvo@unisa.it](mailto:eponticorvo@unisa.it)

Few layer graphene (FLG)/Fe<sub>3</sub>O<sub>4</sub> nanohybrid has been successfully synthesized by an one-step chemical strategy, consisting in the thermolysis of a suitable magnetite precursor in organic solvent in the presence of surfactants and FLG. This way provides experimental easiness and potential low-cost production. Raman spectroscopy, Transmission electron microscopy – Energy dispersive X-ray spectroscopy (TEM-EDS), thermogravimetric analysis coupled with mass spectrometry (TG-DTG-MS) and X-ray diffraction (XRD) were employed for characterization. The nanoparticles with a size of 5 nm, are monodispersed on FLG. The FLG-Fe<sub>3</sub>O<sub>4</sub> hybrid supercapacitor has good electrochemical capacitance performance within potential range from 0 to 1.0 V. The resulting composite exhibited high specific capacitances of 227 F/g and good cyclability in a three-electrode electrochemical cell. The excellent electrochemical performances can be attributed to the high conductivity of FLG as well as to the uniform nano-size of iron oxide dispersed on the support.

### 1. Introduction

Supercapacitors (SC) are considered one of the newest innovations in the field of electrical energy storage. Their performances are mainly due to their high power density, long lifecycle, and bridging function for the power/energy gap between traditional dielectric capacitors (which have high power output) and batteries/fuel cells (which have high energy storage). SCs can be divided into two groups: (i) Electrical double layer capacitor (EDLC), where the capacitance is attributed to the accumulation of charges at the electrode-electrolyte interface. The typical electrode material of EDLC is high surface area carbon, such as activated carbon, carbon fiber and more recently nanocarbons such as carbon nanotubes (Ciambelli et al., 2004; Di Bartolomeo et al., 2009; Sarno et al., 2012a; Sarno et al., 2013b), aerogel, etc. In particular, the successful fabrication of graphene (Sarno et al., 2013a) has inspired large research activity for the development of new graphene-based ultracapacitors (Stoller et al., 2008); (ii) Redox capacitors, where a battery-type oxidation-reduction reaction occurs, leading to the pseudocapacitance. In general, metal oxides are suitable to provide higher energy density for SC than conventional carbon materials and better electrochemical stability than polymer materials. The general requirements for metal oxides in SC application are the following: (1) the oxide should be electronically conductive, (2) the metal can exist in two or more oxidation states that coexist over a continuous range with no phase changes involving irreversible modifications of a 3-dimensional structure. Moreover, rough calculation has indicated that 90% of a superconductor's cost comes from the electrode material, as an example, despite the exceptional properties of ruthenium oxide, its cost is a practical impediment. Many studies have focused on combining RuO<sub>2</sub> with cheap metal oxides to reduce the cost of using precious metals (Wang et al., 2012). As alternative approaches, researchers have put significant effort into finding cheaper and environmentally friendly materials that exhibit electrochemical behaviour similar to RuO<sub>2</sub>, (these alternative materials include MnO<sub>2</sub>, NiO, Fe<sub>3</sub>O<sub>4</sub>, and V<sub>2</sub>O<sub>5</sub>), and to study hybrid capacitors consisting of composites of carbon materials (e.g. nanocarbons, carbon nanotubes, graphene) and metal oxides. The high surface area and conductivity of nanocarbons offer a support for the metal oxide nanoparticles, avoiding their agglomeration and permitting to achieve a better profit of their properties. Fe<sub>3</sub>O<sub>4</sub> is an inexpensive material exhibiting pseudocapacitance. Formerly, low specific capacitance (5.3 F/g in 1 M

Na<sub>2</sub>SO<sub>4</sub> solution) has been reported for Fe<sub>3</sub>O<sub>4</sub> (Wang et al., 2012). More recently, a specific capacitance of 118.2 F/g for a Fe<sub>3</sub>O<sub>4</sub> film in 1M Na<sub>2</sub>SO<sub>4</sub> solution has been reported, with a capacitive retention of 88.8% after 500 charging/discharging cycles (Wang et al., 2012). The highest specific capacitance (185 F/g evaluated at 1mA/cm<sup>2</sup>) for uniform nanosized Fe<sub>3</sub>O<sub>4</sub> nanoparticles in 3M KOH between -1 and 0 volt has been recently reported (Mitchell et al., 2014). Du et al. (Du et al., 2009) prepared an activated carbon-magnetite (AC)/Fe<sub>3</sub>O<sub>4</sub> electrode able to delivery a specific capacitance of 37.9 F/g at a current density of 0.5 mA/cm<sup>2</sup> aiming to improving the specific energy density and limiting the voltage of carbonaceous materials, additionally their initial capacity has been kept at 82% after 500 cycles. Guan et al. in 2013 (Guan et al., 2013) reported an improved specific capacitance and an excellent cyclic stability for their carbon nanotubes-magnetite (CNT)/Fe<sub>3</sub>O<sub>4</sub> in a 6M KOH solution in the potential windows -1–0 volt. In particular, at 10 mA/cm<sup>2</sup> capacitance values of 80.1 F/g, 36.1 F/g and 117.2 F/g for carbon nanotubes, Fe<sub>3</sub>O<sub>4</sub> nanoparticles and CNT/Fe<sub>3</sub>O<sub>4</sub> respectively were found, indicating that the presence of a supporting material can increase the capacitance of a factor of 3.2. Some papers reported results of SC behaviour of Fe<sub>3</sub>O<sub>4</sub> nanoparticles on graphene oxide (GO), even after reduction (rGO). In particular, maximum specific capacitance of 180 F/g in a 1M H<sub>2</sub>SO<sub>4</sub> solution and 65 F/g in a 1M Na<sub>2</sub>SO<sub>4</sub> at 10mV/s, has been obtained for Fe<sub>3</sub>O<sub>4</sub>-functionalized graphene, in the potential windows 0–1 Volt (Mishra et al., 2011). They also found a specific capacitance of 140 F/g in 1M H<sub>2</sub>SO<sub>4</sub> solution at 10 A/g. Qu et al. (Qu et al., 2011) in the window -1–0 Volt in LiOH solution and Shi et al. (Shi et al., 2011) between -0.8–0.2 in 1M KOH, reported high capacitance values in the presence of very high amount of Fe<sub>3</sub>O<sub>4</sub> on rGO. Recently (Wang et al., 2014), a high specific discharge capacitance of 220.1 F/g at 0.5 A/g, that remains stable after 3000 charge/discharge cycles, has been reported for Fe<sub>3</sub>O<sub>4</sub>/rGO (reduced graphene oxide electrode) in 1M KOH between -1.1 and 0 volt. Despite several papers reporting SC data for Fe<sub>3</sub>O<sub>4</sub> on GO, even after reduction (rGO), never results have been reported in the range of 0–1 volts and in H<sub>2</sub>SO<sub>4</sub> solution, regarding Fe<sub>3</sub>O<sub>4</sub> nanoparticles dispersed on the more conductive graphene, obtained by physical exfoliation of graphite (Sarno et al., 2014b). The latter process is inherently less laborious and does not require a large number of chemical reagents and complex procedures, returning few layer graphene sheets with an intact backbone structure, without secondary functionalities, which insertion results in a reduced electrical performances. Nanomaterials can be synthesized by several different methods, among them the “bottom-up” chemical strategies are very fruitful, because they provide experimental easiness and potential low-cost production (Altavilla et al., 2013), together with an excellent synthesis control of monodispersed size nanoparticles. In this paper we want to point out for the first time a novel one-step synthesis strategy for the preparation of few layer graphene nanosheets-magnetite (FLG)/Fe<sub>3</sub>O<sub>4</sub> nanohybrid. Such strategy is based on the thermal decomposition of a magnetite precursor in organic solvent in the presence of surfactants and FLG. This material consists of Fe<sub>3</sub>O<sub>4</sub> nano-sized particles, coated with organic chains, which prevent aggregation and increase the wettability and therefore the dispersion on FLG, obtained by physical exfoliation of graphite. It is worth noticing: (i) we have obtained the highest value of the capacity measured (227 F/g) in presence of a very low amount of Fe<sub>3</sub>O<sub>4</sub> compared with other papers; and (ii) the layers arrangement in FLG, which consists of a certain fraction of monolayers together with more thicker fractions (Sarno et al., 2014b) could open new perspectives for further improvements. Raman Spectroscopy, Transmission Electron Microscopy (TEM), Thermogravimetric analysis coupled with Mass Spectrometry (TG-DTG-MS) and X-ray diffraction (XRD) were employed for characterization. The electrochemical performances of the FLG/Fe<sub>3</sub>O<sub>4</sub> hybrid supercapacitor were investigated by cyclic voltammetry (CV) and galvanostatic charge/discharge tests in 1M H<sub>2</sub>SO<sub>4</sub> solution. The results of CV and the charge/discharge measurements proved that this kind of hybrid supercapacitor has good electrochemical capacitance performance within potential range from 0 to 1 V.

## 2. Experimental

The preparation of magnetite nanoparticles (Sarno et al., 2014a) was carried out using standard airless procedures and commercially available reagents. Absolute ethanol, hexane, and dichloromethane (99%) were used as received. Benzyl ether (99%), 1,2-hexadecanediol (97%), oleic acid (90%), oleylamine (>70%), Iron(III) acetylacetonate were purchased from Aldrich Chemical Co. In particular, Fe(acac)<sub>3</sub> (2 mmol), 1,2-hexadecanediol (10 mmol), oleic acid (6 mmol), oleylamine (6 mmol), and phenyl ether (20 mL) were mixed and magnetically stirred under nitrogen flow. The mixture was heated to 200 °C for 30 min and then, under a blanket of nitrogen, furtherly heated to reflux (265 °C) for 30 min. The formed black-brown mixture was cooled to room temperature by removing the heat source. Under ambient conditions, ethanol (40 mL) was added to the mixture, and a black material was precipitated and separated via centrifugation. The black product was then dissolved in hexane. Centrifugation (6000 rpm, 10 min) was applied to remove any undispersed residue. The nanohybrid were then precipitated with ethanol, centrifuged (6000 rpm, 10 min) to remove the solvent, and redispersed into hexane. The characterization was obtained by different techniques. Transmission electron

microscopy (TEM) images were acquired using a FEI Tecnai electron microscope, equipped with an EDX probe, and operated at 200 KV with a LaB6 filament as source of electrons. Raman spectra were obtained at room temperature with a micro-Raman spectrometer Renishaw inVia with a 514 nm excitation wavelength (laser power 30 mW) in the range 100-3000  $\text{cm}^{-1}$ . XRD measurements were performed with a Bruker D8 X-ray diffractometer using  $\text{CuK}\alpha$  radiation. Thermogravimetric analysis (TG-DTG) at 10 K/min heating rate was performed in flowing air with a SDTQ 600 Analyzer (TA Instruments) coupled with a mass spectrometer.

For the electrochemical measurements 4 mg of catalyst were dispersed in 80  $\mu\text{l}$  of 5 wt% Nafion solution to form a homogeneous ink. Then the catalyst ink was loaded onto a 3 mm diameter glassy carbon electrode. The electrochemical performances of the FLG- $\text{Fe}_3\text{O}_4$  hybrid supercapacitor were investigated by cyclic voltammetry (CV) and galvanostatic charge/discharge tests in 1M  $\text{H}_2\text{SO}_4$  solution in the potential range from 0 to 1.0 V. Saturated calomel, graphite and a loadable glassy carbon electrode were used as the reference electrode, the counter electrode and the working electrode, respectively.

### 3. Results and discussion

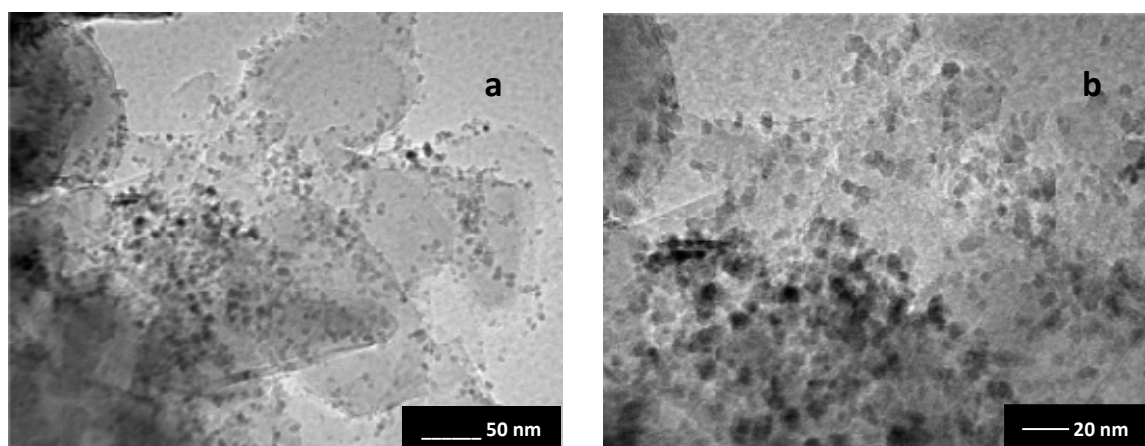


Figure 1: TEM images of FLG/ $\text{Fe}_3\text{O}_4$  (a, b).

TEM images, carried out to provide insights into the morphology of FLG/ $\text{Fe}_3\text{O}_4$  nanohybrid, are reported in Figure 1a and 1b. Figure 1a shows a typical low magnification image of the product, that consists of 5 nm nanoparticles (standard deviation  $\sigma=1.8$  nm), dispersed on FLG preventing agglomeration. The TEM images reveal that the  $\text{Fe}_3\text{O}_4$  nanoparticles are attached to the graphene sheets, even after the ultrasonication used to disperse FLG/ $\text{Fe}_3\text{O}_4$  nanohybrid for TEM characterization. FLG, that were obtained by a physical exfoliation of graphite (Sarno et al., 2014b) have: lateral sizes of few micrometres; a number fraction of monolayer graphene (number of monolayers/total number of flakes) equal to 22%; more than 85% of the total sheets number have layers ranging from 1 to 13; and a fraction of the total sheets number with about 30 layers.

The XRD pattern was used to identify the nanoparticles structure (Figure 2a). All the peak positions at 30.1 (200), 35.4 (311), 43.0 (400), 53.7 (422) 57.2 (511) and 62.6 (440) are consistent with the standard X-ray data of the magnetite phase (Gao et al., 2011; Sun et al., 2009; Zhou et al., 2010). The peaks are broadened as typical of very low particles size. The main particles size measured by using the Scherrer equation (5.1 nm) is close to the TEM results. It means that the as synthesized particles are single crystals. Besides magnetite peaks we did not observe any other oxide peaks in the diffraction pattern. Because the XRD pattern of magnetite and maghemite are very similar, Raman spectroscopy was used to distinguish the different structural phases of iron oxides. Magnetite has the main band centred at  $668\text{ cm}^{-1}$  ( $A_{1g}$ ) (see Figure 2b), no other characteristic iron oxide bands were observed. In the high wavelength range the typical spectrum of FLG is also reported. The two most intense features are the G peak at  $\sim 1570\text{ cm}^{-1}$  and the 2D band at  $\sim 2700\text{ cm}^{-1}$ , which differs from that typical for graphite, consisting of two components  $2D_1$  and  $2D_2$  (the second with higher intensity than the first), has a quite flat apex and can be easily deconvoluted with almost two peaks. A broad D-band can be also seen, likely due to the FLG edges (taking into account the laser spot dimension and the flakes size (Sarno et al., 2014b)). TG-DTG under a flux of  $\text{O}_2$  (2 v/v %) in  $\text{N}_2$  is shown in Figure 3a. From room temperate to  $500^\circ\text{C}$  a weight loss due to organic chains release, see the total ion current (TIC) of the most intense mass fragments peak:  $m/z = 30$  form oleylamine and oleic acid, happens together with a  $\text{CO}_2$  release due to their oxidation in presence of the few percentage of oxygen. The FLG oxidation begins at about  $500^\circ\text{C}$ . TG-DTG measurement in air (Figure 3b) can identify the relative amount of: the coating agents on the

surface of the nanoparticles, FLG and Fe<sub>3</sub>O<sub>4</sub>. The TG curve in Figure 3b display two weight loss processes. The first weight loss, as for the analysis under nitrogen reached flow (Figure 3a), is due to the organic chains and corresponds to about 5 wt.% of the sample. The second weight loss (DTG peak at 645°C) corresponds to FLG oxidation, the TG residue at 900°C (about 21 wt.%) being compatible with the starting amount of FLG and the formation of oxidized magnetite.

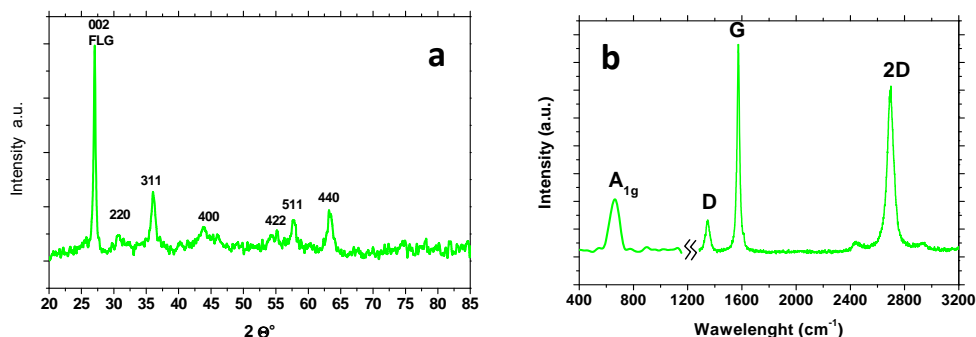


Figure 2: XRD diffraction patterns (a), and Raman spectrum (b) of FLG/Fe<sub>3</sub>O<sub>4</sub> nanohybrid.

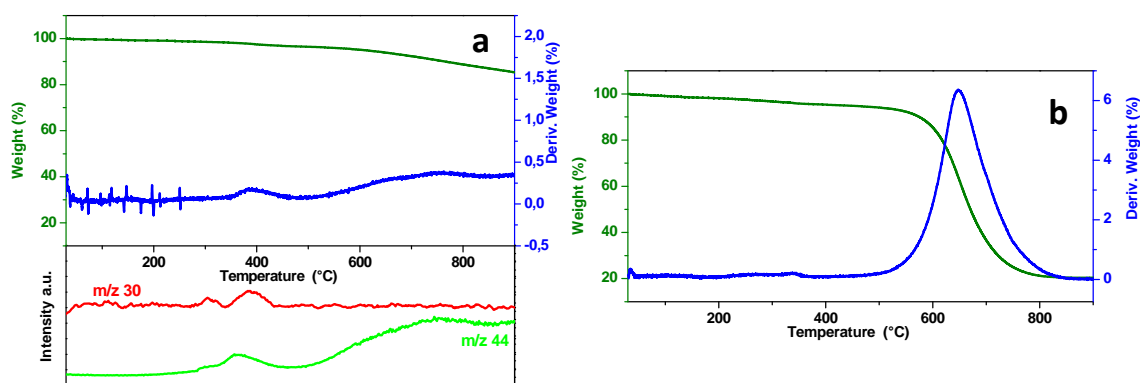


Figure 3: TG-DTG-MS analysis in O<sub>2</sub> (2 v/v %)/N<sub>2</sub> flow (a) and TG-DTG in air (b) of FLG/Fe<sub>3</sub>O<sub>4</sub> nanohybrid.

In order to evaluate the electrochemical properties of FLG/Fe<sub>3</sub>O<sub>4</sub> nanohybrid, cycling voltammetry (CV) and galvanostatic charge/discharge tests were performed. The CV curves at 2-10-20-50-100 mV/s in the potential window of 0–1 V in 1M H<sub>2</sub>SO<sub>4</sub> electrolyte are presented in Figure 4. These curves are not clear rectangular in shape and show a step (i.e. pseudocapacitance) in the range from 0 to 1V. They exhibit quite mirror-image characteristics, which indicate a good capacitive behavior. The specific capacitance was calculated from the discharge curve (Figure 5a, b, c) using the following equation:  $C = (I\Delta t)/(\Delta Vm)$ , where  $C$  is the specific capacitance,  $I$  is the current (A),  $\Delta t$  is the discharge time,  $\Delta V$  the voltage applied and  $m$  is the mass of working electrode. According to the discharge curve, a capacitance of 227 F/g, at a current density of 0.23 A/g, was obtained: (i) with a very low amount of Fe<sub>3</sub>O<sub>4</sub>, if compared with other papers; and (ii) on conductive FLG, which consists of a certain fraction of monolayers together with more thicker fractions, obtained by a simple process that does not require the use of a number of chemical reagents and complex procedure. As could be expected the specific capacitance decreases with the increasing of current density, which originate from the internal resistance of the electrode, to 191 F/g at 0.6 A/g and 180 F/g at 20A/g. The high reported value of capacitance in the present work compared to other reported value may be attributed to the uniform dispersion of magnetite nanoparticles over the surface of FLG.

The capacity retention has been one of the main topic that seemed to hinder the use of Fe<sub>3</sub>O<sub>4</sub> for SC (Wang et al., 2012). However, the problem appears overcome by composite materials in which the nanoparticles are dispersed on nanocarbons (Guan et al., 2013;). Moreover, recently encouraging results were also obtained with nanoparticles alone, characterized by uniform nano-size (Mitchell et al., 2014). Figure 5d shows the long cycle stability of our nanohybrid as evaluated at 20 A/g. The electrode material retains 91% of its initial capacitance after 1000 cycles, indicating a good stability and a long cycle life. The excellent cycling performances of the monohybrid can be attributed to the favourable function of FLG for anchoring nanosized

$\text{Fe}_3\text{O}_4$  particles, which effectively prevents their aggregation. The energy density and power densities can be further calculated from these results (see Figure 5e) using the following equations:  $E = 1/2C(\Delta V)^2$ ,  $P=E/t$ , where  $E$  is the energy density,  $C$  is the specific capacitance,  $\Delta V$  is the potential range,  $P$  is power density and  $t$  is the time to discharge. The nanohybrid reaches an energy density of 63 Wh/kg at a power density of 232 W/Kg, and still remains 50 Wh/kg at a power density of 20000 W/Kg, exhibiting a large power range that can be obtained while maintaining a relatively high energy density. The results illustrate that the nanohybrid have very promising properties for the development of low cost and environmental friendly high performance supercapacitor.

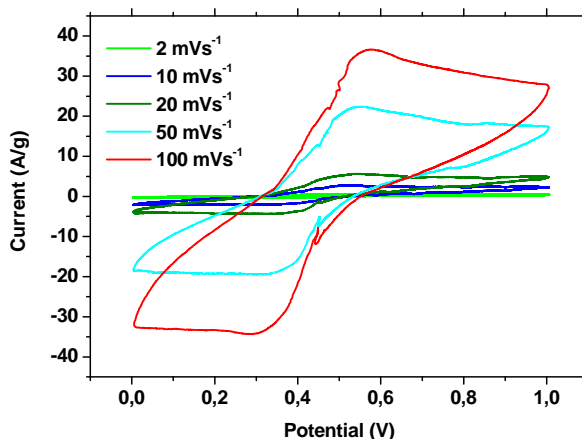


Figure 4 Cyclic voltammetry of the nanohybrid.

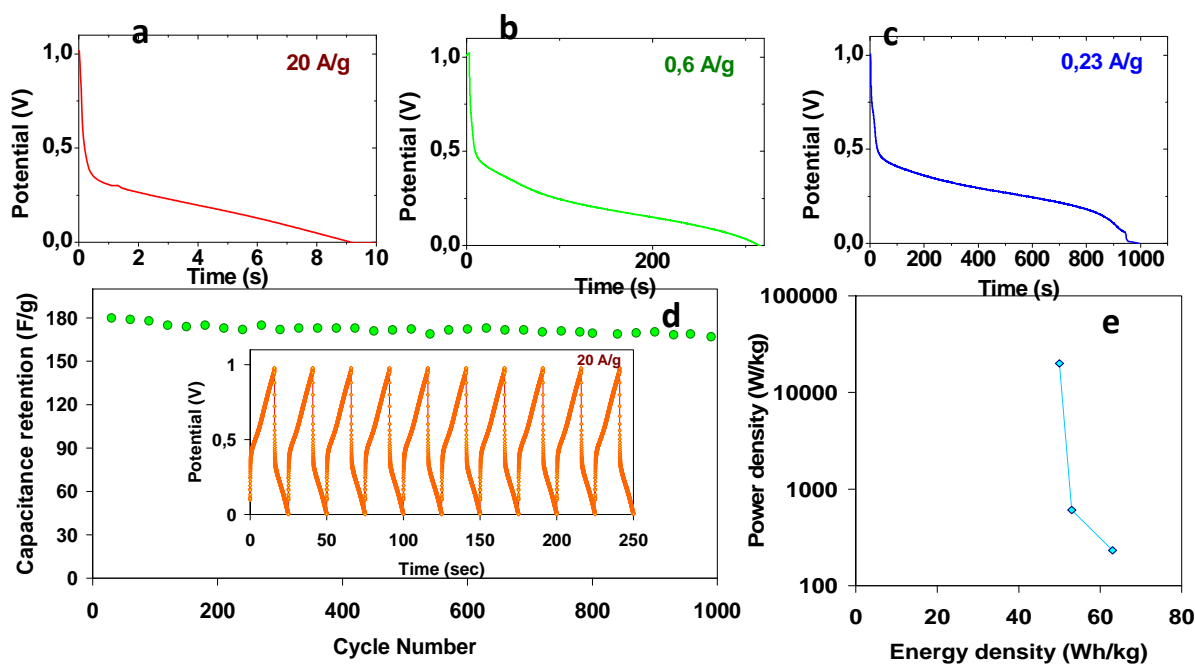


Figure 5 Galvanostatic charge/discharge curves of the nanohybrid at 20 A/g (a), 0.6A/g (b) and 0.23 A/g (c). Capacitance retention at 20 A/g (d).

#### 4. Conclusions

A nanohybrid consisting of  $\text{Fe}_3\text{O}_4$  nano-sized particles, coated with organic chains, which prevent aggregation and increase the wettability and therefore the dispersion on very conductive FLG, obtained by physical exfoliation of graphite, has been prepared by a new and facile one pot synthesis process.

The sample was wide characterized by the combined use of different techniques and tested in the range of 0–1 volts and in H<sub>2</sub>SO<sub>4</sub> solution. It is worth noticing: (i) the highest value of capacity (227 F/g) and good energy and power density performances, if compared with literature results, despite the very low amount of Fe<sub>3</sub>O<sub>4</sub>. Moreover, the layered arrangement of FLG, which consists of a certain fraction of monolayers together with more thicker fractions, can open new perspectives for further improvements.

## References

- Altavilla C., Sarno M., Ciambelli P., Senatore A., Petrone V., 2013, New 'chimie douce' approach to the synthesis of hybrid nanosheets of MoS<sub>2</sub> on CNT and their anti-friction and anti-wear properties, *Nanotechnology*, 24, 125601.
- Ciambelli P., Sannino D., Sarno M., Nagy J.B., 2004, Characterization of nanocarbons produced by CVD of ethylene in alumina or aluminosilicate matrices, *Adv. Eng. Mater.*, 6, 804-811.
- Di Bartolomeo A., Sarno M., Giubileo F., Altavilla C., Iemmo L., Piano S., Bobba F., Longobardi M., Scarfato A., Sannino D., Cucolo A.M., Ciambelli P., 2009, Multiwalled carbon nanotube films as small-sized temperature sensors, *J. Appl. Phys.*, 105, 064518.
- Du X., Wang C., Chen M., Jiao Y., Wang J., 2009, Electrochemical Performances of Nanoparticle Fe<sub>3</sub>O<sub>4</sub>/Activated Carbon Supercapacitor Using KOH Electrolyte Solution, *J. Phys. Chem. C*, 113, 2643-2646.
- Gao M., Li W., Dong J., Zhang Z., Yang B., 2011, Synthesis and Characterization of Superparamagnetic Fe<sub>3</sub>O<sub>4</sub>@SiO<sub>2</sub> Core-Shell Composite Nanoparticles, *World J. Condens. Matter Phys.*, 1, 49-54.
- Guan D., Gao Z., Yang W., Wang J., Yuan Y., Wang B., Zhang M., Liu L., 2013, Hydrothermal synthesis of carbon nanotube/cubic Fe<sub>3</sub>O<sub>4</sub> nanocomposite for enhanced performance supercapacitor electrode material, *Mater. Sci. Eng. B*, 178, 736-743.
- Mishra A.K., Ramaprabhu S., 2011, Functionalized Graphene-Based Nanocomposites for Supercapacitor Application, *J. Phys. Chem. C*, 115, 14006-14013.
- Mitchell E., Gupta R.K., Mensah-Darkwa K., Kumar D., Ramasamy K., Gupta B. K., Kahol P., 2014, Facile synthesis and morphogenesis of superparamagnetic iron oxide nanoparticles for high-performance supercapacitor applications, *New J. Chem.*, 38, 4344-4350.
- Qu Q., Yang S., Feng X., 2011, 2D Sandwich-like Sheets of Iron Oxide Grown on Graphene as High Energy Anode Material for Supercapacitors, *Adv. Mater.*, 23, 5574-5580.
- Sarno M., Cirillo C., Piscitelli R., Ciambelli P., 2013a, A study of the key parameters, including the crucial role of H<sub>2</sub> for uniform graphene growth on Ni foil, *J. Mol. Catal. A: Chem.*, 366, 303-314.
- Sarno M., Sannino D., Leone C., Ciambelli P., 2012a, Evaluating the effects of operating conditions on the quantity, quality and catalyzed growth mechanisms of CNTs, *J. Mol. Catal. A: Chem.* 357, 26-38.
- Sarno M., Tamburrano A., Arurault L., Fontorbes S., Pantani R., Datas L., Ciambelli P., Sarto M.S., 2013b, Electrical conductivity of carbon nanotubes grown inside a mesoporous anodic aluminium oxide membrane, *Carbon*, 55, 10-22.
- Sarno M., Cirillo C., Ciambelli P., 2014a, Selective graphene covering of monodispersed magnetic nanoparticles, *Chem. Eng. J.* 246, 27-38.
- Sarno M., Garamella A., Cirillo C., Ciambelli P., 2014b, MoS<sub>2</sub>/MoO<sub>2</sub>/Graphene Electrocatalyst for HER, *Chemical Engineering Transaction*, 41, 385-390. DOI: 10.3303/CET1441065
- Shi W., Zhu J., Sim D.H., Tay Y.Y., Lu Z., Zhang X., Sharma Y., Srinivasan M., Zhang H., Hng H.H., Yan Q., 2011, Achieving high specific charge capacitances in Fe<sub>3</sub>O<sub>4</sub>/reduced graphene oxide nanocomposites, *J. Mater. Chem.*, 21, 3422-3427.
- Stoller M.D., Park S., Zhu Y., An J., Ruoff R.S., 2008, Graphene-Based Ultracapacitors, *Nano Lett.*, 8, 3498-3502.
- Sun X., Zheng C., Zhang F., Yang Y., Wu G., Yu A., Guan N., 2009, Size-Controlled Synthesis of Magnetite (Fe<sub>3</sub>O<sub>4</sub>) Nanoparticles Coated with Glucose and Gluconic Acid from a Single Fe(III) Precursor by a Sucrose Bifunctional Hydrothermal Method, *J. Phys. Chem. C*, 113, 16002-16008.
- Wang G., Zhang L., Zhang J., 2012, A review of electrode materials for electrochemical supercapacitors, *Chem. Soc. Rev.*, 41, 797-828.
- Wang Q., Jiao L., Du H., Wang Y., Yuan H., 2014, Fe<sub>3</sub>O<sub>4</sub> nanoparticles grown on graphene as advanced electrode materials for supercapacitors, *J. Power Sources*, 245, 101-106.
- Zhou G., Wang D.-W., Li F., Zhang L., Li N., Wu Z.-S., Wen L., Qing L.G., Cheng H.-M., 2010, Graphene-Wrapped Fe<sub>3</sub>O<sub>4</sub> Anode Material with Improved Reversible Capacity and Cyclic Stability for Lithium Ion Batteries, *Chem. Mater.*, 22, 5306-5313.